Virology 527 (2019) 21–31

Contents lists available at ScienceDirect

Virology

journal homepage: www.elsevier.com/locate/virology

Polymorphisms of the cytidine deaminase APOBEC3F have different HIV-1 restriction efficiencies

Nazanin Mohammadzadeh[a], Tyson B. Follack[a], Robin P. Love[a], Kris Stewart[b,c,d], Stephen Sanche[b,d], Linda Chelico[a,d,*]

[a] University of Saskatchewan, Biochemistry, Microbiology, and Immunology, College of Medicine, Saskatoon, Saskatchewan, Canada
[b] University of Saskatchewan, Department of Medicine, College of Medicine, Saskatoon, Saskatchewan Canada
[c] Saskatchewan Infectious Disease Care Network, Saskatoon, Saskatchewan, Canada
[d] Saskatchewan HIV/AIDS Research Endeavour, Saskatoon, Saskatchewan, Canada

ARTICLE INFO

Keywords:
HIV-1
APOBEC3
Vif
Restriction factors
Infectivity
Deamination
Mutagenesis

ABSTRACT

The APOBEC3 enzyme family are host restriction factors that induce mutagenesis of HIV-1 proviral genomes through the deamination of cytosine to form uracil in nascent single-stranded (-)DNA. HIV-1 suppresses APOBEC3 activity through the HIV-1 protein Vif that induces APOBEC3 degradation. Here we compared two common polymorphisms of APOBEC3F. We found that although both polymorphisms have HIV-1 restriction activity, APOBEC3F 108 A/231V can restrict HIV-1 ΔVif up to 4-fold more than APOBEC3F 108 S/231I and is partially protected from Vif-mediated degradation. This resulted from higher levels of steady state expression of APOBEC3F 108 A/231 V. Individuals are commonly heterozygous for the APOBEC3F polymorphisms and these polymorphisms formed in cells, independent of RNA, hetero-oligomers between each other and with APOBEC3G. Hetero-oligomerization with APOBEC3F 108 A/231V resulted in partial stabilization of APOBEC3F 108 S/231I and APOBEC3G in the presence of Vif. These data demonstrate functional outcomes of APOBEC3 polymorphisms and hetero-oligomerization that affect HIV-1 restriction.

1. Introduction

APOBEC3 (A3) enzymes are a family of deoxycytidine deaminases that can act as host restriction factors for HIV-1 (Feng et al., 2014; Harris et al., 2012). The A3 enzymes deaminate cytosine in single-stranded (ss) DNA to form uracil (Harris et al., 2003, 2002; Mangeat et al., 2003; Zhang et al., 2003). Of the seven human A3 enzymes, there are five that can restrict the replication of HIV-1 in CD4 + T cells through the formation of uracils in (-) strand proviral DNA. These enzymes, A3D, A3F, A3G, A3H (haplotypes II, V, and VII), and A3C (S188I) restrict HIV-1 with varying efficiencies (Adolph et al., 2017; Hultquist et al., 2011; Liddament et al., 2004; OhAinle et al., 2008; Sheehy et al., 2002; Wiegand et al., 2004; Wittkopp et al., 2016; Zheng et al., 2004). In an HIV-1 infected CD4 + T cell, these enzymes can become encapsidated into assembling virions through an interaction with cellular or HIV-1 genomic RNA that is also bound to HIV-1 Gag (Apolonia et al., 2015; York et al., 2016). After virion maturation and infection of a target cell, the encapsidated A3 enzymes can access single-stranded HIV-1 (-) DNA when it is synthesized and exposed through reverse transcription and RNase H activity (Yu et al., 2004). The cytosines that become deaminated to uracil are copied by the reverse transcriptase during (+) DNA synthesis and result in guanine to adenine (G→A) mutations on the coding strand (Harris et al., 2003, 2002; Mangeat et al., 2003; Yu et al., 2004; Zhang et al., 2003). These mutations can induce DNA repair enzyme-mediated degradation of proviral DNA or result in functional inactivation of integrated proviral DNA (Harris and Dudley, 2015). HIV-1 Vif suppresses the encapsidation and activity of A3 enzymes by mediating their polyubiquitination and proteasomal degradation (Conticello et al., 2003; Kao et al., 2003; Mariani et al., 2003; Marin et al., 2003; Sheehy et al., 2003; Stopak et al., 2003; Yu et al., 2003). HIV-1 Vif hijacks a Cullin 5 E3 ubiquitin ligase complex and acts as the substrate receptor by replacing the host protein SOCS2 (Yu et al., 2003). This enables HIV-1 Vif to interact directly with components of the ubiquitin ligase complex, Elongin C and Cullin 5 (Guo et al., 2014). HIV-1 Vif can also directly interact with A3D, A3F, A3G, A3H, and A3C, which induces their ubiquitination and proteasomal degradation (Kitamura et al., 2012; Mangeat et al., 2004; Schrofelbauer et al., 2004; Xu et al., 2004). Obligatory for stability, Vif also interacts with the transcription cofactor CBF-β (Jager et al., 2012; Zhang et al., 2011).

* Corresponding author at: University of Saskatchewan, Biochemistry, Microbiology, and Immunology, College of Medicine, Saskatoon, Saskatchewan, Canada.
E-mail address: linda.chelico@usask.ca (L. Chelico).

https://doi.org/10.1016/j.virol.2018.11.004
Received 25 September 2018; Received in revised form 3 November 2018; Accepted 4 November 2018
Available online 15 November 2018

Despite the presence of Vif, A3 enzymes are still able to be encapsidated into HIV-1 virions and induce mutagenesis (Bruner et al., 2016; de Lima-Stein et al., 2014; Eyzaguirre et al., 2013; Janini et al., 2001; Kieffer et al., 2005; Land et al., 2008; Pace et al., 2006; Pathak and Temin, 1990; Piantadosi et al., 2009; Vartanian et al., 2002, 1991, 1994). Although translation of Vif mRNA results in high levels of Vif in cells before virus particle assembly, which depletes A3s from infected CD4 + T cells, the induced degradation of A3s is not complete (Holmes et al., 2015). Evidence of this comes from high levels of A3 induced stop codons and missense mutations in HIV-1 proviral DNA in acute and chronic proviral DNA isolated from HIV-1 + individuals (Bruner et al., 2016). Sequencing of integrated proviral genomes from multiple studies have revealed that the mutations are present on the (+) DNA in both 5′GG→5′AG and 5′GA→5′AA contexts (Bruner et al., 2016; de Lima-Stein et al., 2014; Eyzaguirre et al., 2013; Janini et al., 2001; Kieffer et al., 2005; Land et al., 2008; Ooms et al., 2013; Pace et al., 2006; Pathak and Temin, 1990; Piantadosi et al., 2009; Vartanian et al., 2002, 1991, 1994). Mutations in the 5′GG context originate primarily from A3G that deaminates preferentially in 5′ CCA motifs on the (-) DNA (underlined C deaminated) (Yu et al., 2004). This sequence context most often results in mutations that introduce stop codons and mutations at glycines (Adolph et al., 2018). Mutations in the 5′GA context originate primarily from A3D, A3F, A3H, and A3C (S188I) due to a preference to deaminate in 5′TC motifs on the (-) DNA (Dang et al., 2006; Langlois et al., 2005; Liddament et al., 2004; Ooms et al., 2013). Mutations at the 5′TC motif can also introduce stop codons and missense mutations in a wider variety of amino acids (Adolph et al., 2018). The fate of these mutations may inactivate HIV-1 or may lead to evolution in various forms, such as drug resistance, CTL escape, and changes in co-receptor usage (Alteri et al., 2015; Grant and Larijani, 2017; Kim et al., 2014; Mulder et al., 2008; Pollack et al., 2017; Sato et al., 2014). However, depending on the experimental system some studies have found that A3 enzymes do not contribute to drug resistance and may enhance CTL recognition (Delviks-Frankenberry et al., 2016; Jern et al., 2009; Monajemi et al., 2014; Pollack et al., 2017; Squires et al., 2015). Although A3G is the most active deaminase in a ΔVif HIV-1 infection, it is also very sensitive to Vif (Ara et al., 2014; Baig et al., 2014; Chaipan et al., 2013). Thus, despite there being lower activity from A3D and A3F in ΔVif HIV-1 infections, there is some evidence that A3F is less sensitive to Vif, and as a result, may be a greater contributor to mutagenesis during HIV-1 infections in vivo (An et al., 2016; Ara et al., 2014; Duggal et al., 2011; Hultquist et al., 2011; Zennou and Bieniasz, 2006). There is also evidence that in chronically infected individuals that HIV-1 Vif can acquire mutations that result in partial activity, thereby enabling A3 encapsidation and mutagenesis (Simon et al., 2005). However, it is unlikely that these mutations in Vif are acquired early in infection and since A3-mediated mutagenesis is found in acute infections, the data suggest that other mechanisms can enable A3 encapsidation in the presence of Vif (Bruner et al., 2016).

Resistance to Vif mediated degradation has been characterized for some A3 enzymes. A3H exists as seven major haplotypes in humans with different protein stability, HIV-1 restriction ability, and sensitivity to Vif (OhAinle et al., 2008; Ooms et al., 2010; Wang et al., 2011). These haplotypes result from a combination of five different single-nucleotide polymorphisms (SNPs) (OhAinle et al., 2008; Ooms et al., 2010; Wang et al., 2011). The diversity of A3H in the human population necessitates constant adaptation of HIV-1 Vif to A3H, especially since stable and restrictive A3H haplotypes (II, V, and VII) show population stratifications (OhAinle et al., 2008; Ooms et al., 2013; Wang et al., 2011). These dynamics result in a situation where A3H can act as a transmission barrier for some HIV-1 strains that do not have a Vif capable of inducing A3H degradation (Refsland et al., 2014). At the very least, this A3H resistance to some HIV-1 Vifs can increase the time until CD4 + T cell counts decrease or until the development of AIDS, while Vif acquires the adaptive mutations to overcome A3H (Ooms et al., 2013). The number of SNPs in other A3s is significantly lower and most commonly they have been found to result in inactivation of the A3 or no effect (An et al., 2004; Duggal et al., 2013; Reddy et al., 2016). Exceptions are A3D and A3C in which SNPs have resulted in increased activity (Adolph et al., 2017; Duggal et al., 2013; Wittkopp et al., 2016). Interestingly, despite cell based assays not uncovering differences in a common variant of A3F A108S/V231I, a population based analysis of multiple pre-treatment cohorts of HIV-1 + individuals showed that the A3F 231V variant was associated with lower viral loads and slower rate of progression to AIDS (An et al., 2016; Duggal et al., 2013; Mulder et al., 2010). The authors suggested that the 231V polymorphism might increase resistance to Vif (An et al., 2016). Despite this amino acid not being within the canonical Vif binding interface on A3F, this observation was also previously reported for A3F 108 A/231V (Albin et al., 2010b; Liddament et al., 2004; Nakashima et al., 2016; Richards et al., 2015; Smith and Pathak, 2010).

Here we assessed the A3F 108 S/231I and A3F 108 A/231V variants for their ability to restrict HIV-1 replication in the presence and absence of Vif. Based on past evidence that A3F can interact with itself and A3G, in an RNA-independent manner (Ara et al., 2017), we assessed how each A3F variant restricted HIV-1 replication when expressed together and in the presence of A3G. Notably, the SNPs responsible for the A3F 108 A/231V and 108 S/231I variants (rs202390, rs2076101) have been identified to commonly occur together in genetic studies (Duggal et al., 2013; Mulder et al., 2010). Further, analysis of multiple human populations from the Ensembl genome browser (release 94) showed that these SNPs are in high linkage disequilibrium ($r^2 > 0.95$) for European, South Asian, and East Asian populations and linkage disequilibrium also occurs, but at lower frequencies, for Mixed American ($r^2 > 0.87$) and African ($r^2 > 0.35$) populations (Zerbino et al., 2018). As a result, we refer to these variants as A3F 231V or A3F 231I for brevity and because this specific variation was correlated epidemiologically in affecting HIV-1 progression (An et al., 2016; Duggal et al., 2013; Mulder et al., 2010). Our analysis of these A3F variants found that the A3F 231V is a more efficient restriction factor for HIV-1 than A3F 231I. The increased restriction was due to an increase in A3F steady state levels in cells. This increased steady state level of A3F 231V resulted in a partial protection from Vif-mediated degradation. Notably, population analysis demonstrated that the A3F 231V and A3F 231I alleles occurred most often together, rather than the homozygous alleles. This appeared to have a functional benefit since the interaction of A3F 231V could also increase the Vif resistance of A3F 231I and A3G, providing a possible reasoning for how high numbers of A3 induced mutations may be acquired in HIV-1 + individuals.

2. Results

2.1. A3F 231V more efficiently restricts HIV-1 infection than A3F 231I

The A3F 231V allele has been shown to be protective in HIV-1 + individuals, but the reason for this was not fully explored (An et al., 2016). Here we conducted an assessment of the HIV-1 restriction ability of A3F 231V and A3F 231I. The effect of untagged A3F 231V and A3F 231I on VSV-G pseudotyped ΔVif HIV-1 infectivity was assessed using transient transfection of different amounts of A3F vector in single-cycle replication assays. Over a range of A3F plasmid transfection amounts, the A3F 231V restricted ΔVif HIV-1 1.4-fold (25 ng, $p \leq 0.05$), 1.6-fold (50 ng, $p \leq 0.01$), and 4.0-fold (100 ng, $p \leq 0.001$) more than A3F 231I (Fig. 1A). Overall the ability for A3F to restrict ΔVif HIV-1 was still 1.5-fold (25 ng, $p \leq 0.01$), 1.8-fold (50 ng, $p \leq 0.01$), and 13.6-fold (100 ng, $p \leq 0.001$) less than A3G, for the more active A3F 231V variant, consistent with previous reports (Fig. 1A) (Hultquist et al., 2011). Also consistent with A3F 231V being protective in HIV-1 + individuals (An et al., 2016), the A3F 231V enabled modest restriction of virus replication in the presence of Vif, which was not observed for A3F 231I or A3G (Fig. 1B, $p \leq 0.01$ for 50 ng and 100 ng).

To confirm that decreases in infectivity in the presence and absence

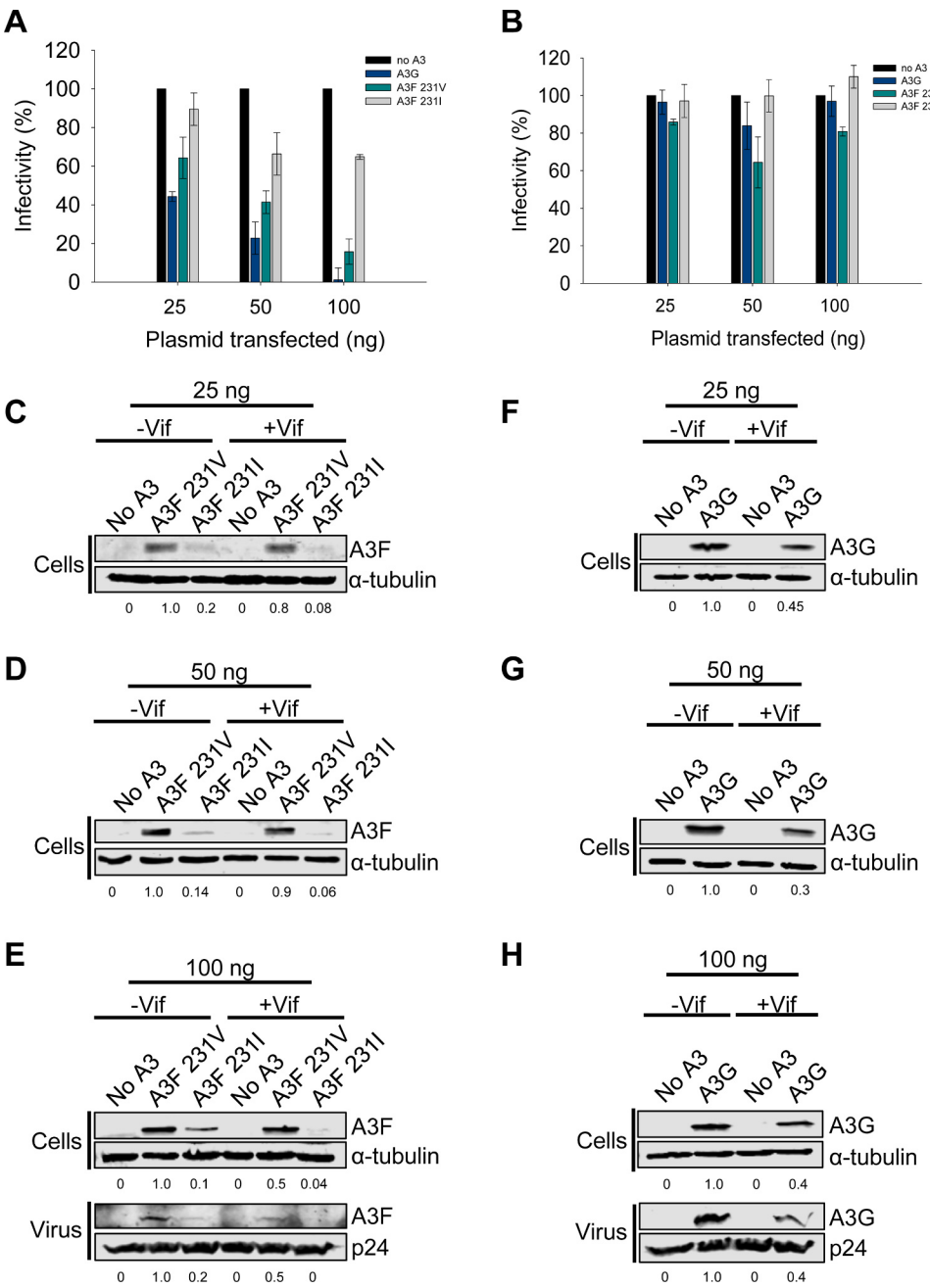

Fig. 1. A3F 231V and A3F 231I have different HIV-1 restriction abilities. (A) Infectivity was measured by β-galactosidase activity in reporter cells infected with HIV-1 ΔVif that was produced in the absence or presence of untagged A3G, A3F 231 V or A3F 231I. Results were normalized to the no A3 condition. (B) Infectivity was measured by β-galactosidase activity in reporter cells infected with HIV-1 + Vif that was produced in the absence or presence of untagged A3G, A3F 231 V or A3F 231I. Results were normalized to the no A3 condition. (A-B) Error bars represent the standard deviations of the mean calculated from three independent experiments. (C-E) Immunoblotting with A3F native antibody was used to detect (C) 25 ng (D) 50 ng and (E) 100 ng transfected A3F expressed in (C-E) cells and (E) encapsidated into HIV-1 virions in -Vif and + Vif conditions. (F-H) Immunoblotting with A3G native antibody was used to detect (F) 25 ng (G) 50 ng and (H) 100 ng transfected A3G expressed in (F-H) cells and (H) encapsidated into HIV-1 virions in -Vif and + Vif conditions. The cell lysate and virion loading controls were α-tubulin and p24, respectively. (C-H) One representative blot from three independent experiments is shown. The A3 expression levels shown below blots were calculated by setting a –Vif condition to 1.0 and determining the relative values of other lanes.

of Vif correlated with virion encapsidation of the A3 enzymes, the cell lysates and virions from the replication assays were analyzed after proteins were resolved by SDS-PAGE and transferred to membranes for immunoblotting. The native antibody used to detect A3F was only able to detect cellular expression (Fig. 1C-E) and not virion encapsidation, except at the 100 ng transfection amount (Fig. 1E and data not shown). These blots showed that the A3F 231 V had a higher steady state expression level than A3F 231I in the absence of Vif (5- to 10- fold) and presence of Vif (10- to 15- fold) (Fig. 1C-E), consistent with higher decreases in HIV-1 infectivity in both of these conditions (Fig. 1A-B). At the highest plasmid transfection amount (100 ng), the A3F variants could be detected in the virus particles. The A3F 231 V was encapsidated 5-fold more than A3F 231I in the absence of Vif and in the presence of Vif encapsidation of the A3F 231 V, but not the A3F 231I was detected (Fig. 1E). Collectively, these data suggest that the A3F 231 V is partially protected from Vif-mediated degradation. Similar limitations with a native antibody for A3G were identified in that the cellular expression levels were detected with the native antibody, but the encapsidation was not detected until the plasmid transfection amount reached 100 ng, despite evidence of HIV-1 restriction in the single-cycle replication assays (Fig. 1A and F-H). Although significant amounts of A3G were detected in the virus in the presence of Vif at the higher transfection amount (Fig. 1H), there was no observable decrease in infectivity (Fig. 1B), presumably due to Vif-mediated inhibition of A3G catalytic activity and processivity that has been previously characterized (Britan-Rosich et al., 2011; Feng et al., 2013).

To investigate further if the A3F 231 V was partially resistant to Vif-mediated degradation we used V5-tagged A3F 231 V and A3F 231I constructs. The tags were used to avoid any possible recognition differences by the native antibody, which recognizes unknown epitopes in the C-terminal half, and to facilitate quantification of immunoblots at lower plasmid transfection amounts. We repeated the experiment in Fig. 1D using 50 ng of V5-tagged A3F expression plasmid in the presence or absence of Vif during a single-cycle replication experiment.

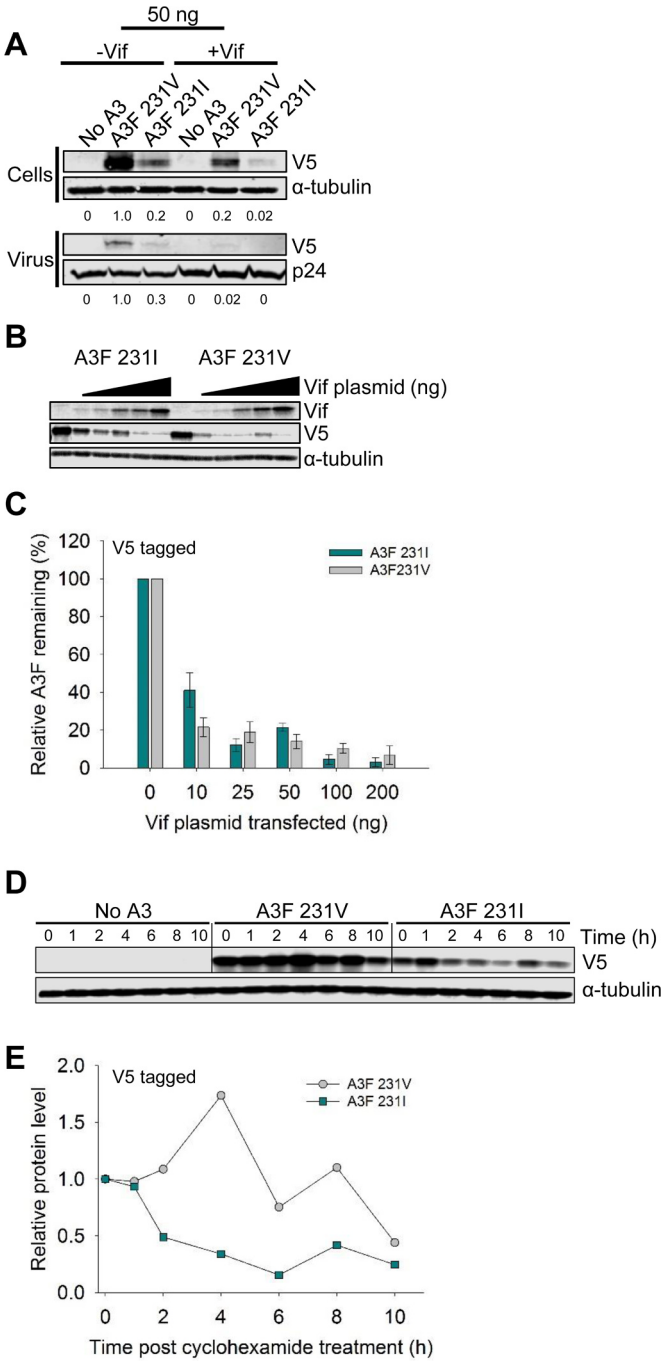

Fig. 2. Differences in steady state expression levels of A3F 231V and A3F 231I influences sensitivity to Vif-mediated degradation. (A) Immunoblotting with V5 antibody after 50 ng of expression plasmid was transfected into 293 T cells in the presence of ΔVif HIV-1 or HIV-1 to detect A3F 231V-V5 and A3F 231I-V5 in cells and encapsidated into HIV-1 virions in -Vif and +Vif conditions. (B) A3F 231V-V5 and A3F 231I-V5 plasmids were transfected into 293 T cells with amounts that resulted in equal steady state expression levels. Increasing amounts of Vif were cotransfected. The amount of Vif-mediated degradation was detected by analysing the intensity of the bands detected with antibody to the V5 tag. One representative blot from three independent experiments is shown. (C) Quantified intensities of the bands from immunoblotting in (B) are shown. Error bars represent the standard deviations of the mean calculated from three independent experiments. (D) Immunoblotting with V5 antibody after 50 ng of expression plasmid was transfected into 293 T cells to detect A3F 231V-V5 and A3F 231I-V5 after cycloheximide treatment. (E) Quantification of the protein levels after cycloheximide treatment showed differences in the stability of A3F 231V-V5 and A3F 231I-V5.

The V5-tagged A3F-231V had the same features as the untagged enzyme, a steady state expression level 5-fold more than the V5-tagged A3F-231I in the absence of Vif and partial resistance to Vif-mediated degradation, in contrast to V5-tagged A3F-231I (Fig. 2A). The higher steady state levels of the A3F 231 V also resulted in higher levels of virion encapsidation in comparison to the A3F 231I, in the presence and absence of Vif (Fig. 2A). Having established that the higher steady state levels of A3F 231 V were indeed due to protein levels in cells and not differences in antibody recognition, we used the V5-tagged constructs to address the basis for the A3F 231 V partial protection from Vif-mediated degradation. We transfected different plasmid amounts of the V5-tagged A3F variants that resulted in approximately equal steady state cellular expression. Using 10 ng of A3F 231V-V5 plasmid and 50 ng of A3F 231I-V5 plasmid, we cotransfected increasing amounts of Vif from an expression vector. Quantification of the immunoblot demonstrated that at these transfection amounts, in the absence of Vif, the steady state levels of both A3F 231V-V5 and A3F 231I-V5 were similar (Fig. 2B). With increasing amounts of transfected Vif, the induced degradation of both A3F variants were also similar (Fig. 2B-C). Thus, the partial protection from Vif observed in Fig. 2A and Fig. 1C-E was not due to an inherent biochemical property of the A3F 231 V, but rather the data suggest that the partial protection from Vif-mediated degradation was due to a higher steady state level of A3F 231 V that exceeded Vif degradation capacity. Consistent with this line of reasoning, we observed stability differences between A3F 231V-V5 and A3F 231I-V5 after cyclohexamide treatment of transfected cells (Fig. 2D-E, 50 ng plasmid transfected for each A3F variant). The A3F 231 V steady state protein levels decreased 2-fold 10 h after cycloheximide treatment (Fig. 2D-E). In contrast, the A3F 231I steady state protein levels decreased 2-fold within 2 h after cycloheximide treatment and continued to decrease through the time course with an ultimate 4-fold decrease in protein levels (Fig. 2D–E).

2.2. A3F 231V induces more mutations than A3F 231I in HIV-1 proviral DNA

We PCR amplified a 351 bp region of HIV-1 *protease* for sequencing under the conditions shown in Fig. 1A (untagged A3s, 50 ng transfection amount) to determine the G→A mutations induced by A3F 231 V and A3F 231I. We observed that in the absence of Vif that G→A mutations per kb were 2.46 for A3F 231 V and 1.42 for A3F 231I (Table 1). The mutations were primarily in the A3F mutation context (Table 1, GA→AA). This ~2-fold difference in mutations is consistent with the decrease in infectivity (Fig. 1A, 50 ng). However, both A3F variants were still less able to induce mutations than A3G (Table 1, 13.5 G→A mutations/kb). This, at least 5-fold, difference in A3F and A3G induced mutations was consistent with previous data and has been found to be due to differences in enzyme processivity (Ara et al., 2014). As a result, these data emphasize the importance of the inherent biochemical characteristics in restriction capacity between A3s. However, when comparing A3F variants, the level of encapsidation appeared to be a determining factor that could increase A3F restriction efficiency for HIV-1 (Table 1, Figs. 1E, and 2A).

Importantly in the presence of Vif, the number of A3-induced mutations by A3F 231 V and A3G were less disparate. A3G did not show significant restriction in the presence of Vif and accordingly induced 36-fold less mutations than in the absence of Vif (Table 1, 0.37 G→A mutations/kb). Consistent with the ability to partially avoid Vif-mediated degradation, the A3F 231 V only had a 4.8-fold decrease in induced mutations (Table 1, 0.51 G→A mutations/kb). Thus, in the presence of Vif the A3F 231 V induced mutations were 1.4-fold more than A3G (Table 1). In the presence of Vif, the A3F 231I induced mutations decreased 11-fold to 0.13 G→A mutations/kb, resulting in 2.3-fold less mutations than A3G and 4-fold less mutations than A3F 231 V (Table 1).

Table 1
Analysis of A3-induced mutagenesis in HIV-1 proviral DNA.

Virus Condition	A3 enzyme	Base pairs sequenced	G→A mutations (total)	GG→AG mutations (total)	GA→AA mutations (total)	G→A Mutations (per kb)	GG→AG mutations (per kb)	GA→AA mutations (per kb)
-Vif	No A3	7722	2	0	0	0.26	0	0
	A3F 231V	7722	19	2	14	2.46	0.26	1.81
	A3F 231I	7020	10	2	6	1.42	0.28	0.85
	A3G	6669	90	83	5	13.5	12.5	0.75
+Vif	No A3	15795	3	0	1	0.19	0	0.06
	A3F 231V	15795	8	0	5	0.51	0	0.32
	A3F 231I	15093	2	0	2	0.13	0	0.13
	A3G	16142	6	4	1	0.37	0.24	0.06

A 351 bp region of HIV-1 *protease* was PCR amplified from the three independent single-cycle replication assays shown in Fig. 1. Clones were sequenced, aligned with Clustal Omega (Sievers et al., 2011), and analyzed using Hypermut (Rose and Korber, 2000).

2.3. A3F genotypes are commonly heterozygous

Since the A3F variants showed different abilities to restrict HIV-1 and different steady state expression levels, we were interested to determine how often in the human population these different variant alleles were heterozygous or homozygous. This was of interest since we have previously shown that A3G and A3F can hetero-oligomerize in the absence of RNA (Ara et al., 2017). If the A3F variants were expressed in the same cell and hetero-oligomerized, the A3F expression levels and restriction ability could potentially be altered.

We obtained genotype data for the corresponding SNP (rs2076101) that results in the 231 V/I polymorphism from Ensembl (release 94) (Zerbino et al., 2018). The cumulative allele data from people of African, Mixed American, East Asian, European and South Asian populations showed that there was an equal frequency of the GTC (G) allele that resulted in the 231 V polymorphism and ATC (A) allele that resulted in the 231I polymorphism (Table 2). Per population, the allelic frequencies varied, with only the European (EUR) population having an approximately equal frequency of the G and A alleles (Table 2). The Mixed American (AMR) and South Asian (SAS) were similar having approximately a 0.40 frequency of the G allele (Table 2). The African (AFR) and East Asian (EAS) populations were biased for one allele, with AFR populations having a 0.81 frequency of the G and EAS having a 0.71 frequency of the A (Table 2). Despite these differences in allelic frequencies, there were high frequencies across all populations of the heterozygous genotype (G/A). The average frequency across all populations for the heterozygous genotype was 0.42 and was similar to the individual genotype frequencies of the EUR, AMR, EAS, and SAS populations (Table 2). Even the AFR population with the lowest allele frequency of the A (0.04), had a G/A genotype frequency of 0.30 (Table 2). These data demonstrate that for many populations, the heterozygotic genotype is dominant. The exceptions are the AFR population where the G/G genotype is dominant (0.66) and the EAS population where the A/A genotype is dominant (0.50) (Table 2).

Table 2
Population analysis of alleles and genotype of A3F SNP rs2076101 that results in A3F 231 V/I.

Population[a]	Allele frequency (G/A)[b]	Genotype frequency
ALL	0.50/0.50	G/G: 0.29 A/A: 0.28 G/A: 0.42
AFR	0.81/0.19	G/G: 0.66 A/A: 0.04 G/A: 0.30
EUR	0.51/0.49	G/G: 0.29 A/A: 0.27 G/A: 0.45
AMR	0.38/0.62	G/G: 0.14 A/A: 0.38 G/A: 0.49
EAS	0.29/0.71	G/G: 0.07 A/A: 0.50 G/A: 0.43
SAS	0.39/0.61	G/G: 0.14 A/A: 0.35 G/A: 0.51

Data were obtained from Ensembl genome browser (release 94) (Zerbino et al., 2018).

[a] Populations are abbreviated as All (ALL), African (AFR), European (EUR), Mixed American (AMR), East Asian (EAS), and South Asian (SAS).

[b] The A3F SNP rs2076101 is a G to A change that codes for A3F 231 V (G) or A3F 231I (A).

2.4. A3F 231V and A3F 231I hetero-oligomerize with each other and A3G

Based on these results showing that different A3F variants can be coexpressed within an individual, we determined whether the A3F variants could hetero-oligomerize with each other or A3G. A3F has been shown to form homo-oligomers and to hetero-oligomerize with A3G, in the absence of RNA (Ara et al., 2017). To determine oligomerization, we used a cotransfection scheme where one A3 had an HA-tag and the other A3 had a V5-tag and determined if one A3 could co-immunoprecipitate the other A3. To ensure uniform co-expression of A3s on a per cell basis we used the pVIVO2 plasmid that has two transcription units within a single vector (see Materials and Methods) (Ara et al., 2017). We used the V5-tagged A3 to immunoprecipitate the binding partner, in the presence of RNase A, and found through blotting for HA that A3G-HA can interact with A3F 231I-V5, as shown previously (Fig. 3) (Ara et al., 2017). We also determined that A3G-HA can interact with A3F 231V-V5 and that A3F 231V-HA can interact with A3F 231I-V5 (Fig. 3).

2.5. A3F 231V promotes higher steady state levels of A3F 231I and A3G

Using the same pVIVO2 expression vectors that were used for the co-immunoprecipitations we conducted single-cycle replication assays to assess if combined expression changed the HIV-1 restriction capability of the coexpressing A3s compared to the individual enzymes. To facilitate immunoblotting of the samples resulting from the infectivity assays, we transfected tagged versions of the A3 enzymes (50 ng) using a combination of HA- and V5- tags so that each A3 was discernable by immunoblotting. The A3G was always HA-tagged, A3F 231I was always V5-tagged and the A3F 231 V was HA- or V5- tagged depending on whether it was coexpressed with A3G or A3F. In the absence of Vif, the A3G-HA alone and A3G-HA/A3F 231V-V5 decreased the infectivity similarly (Fig. 4A). The A3G-HA/A3F 231I-V5 coexpression also decreased HIV-1 infectivity, but the restriction was 3-fold less than the A3G-HA/A3F 231V-V5 restriction, although this was not a statistically significant difference (Fig. 4A). However, both A3F 231I-V5 and A3F 231V-V5 alone restricted the replication of HIV-1 ΔVif 3-fold ($p \leq 0.001$) and 6-fold ($p \leq 0.001$) less, respectively, than when in

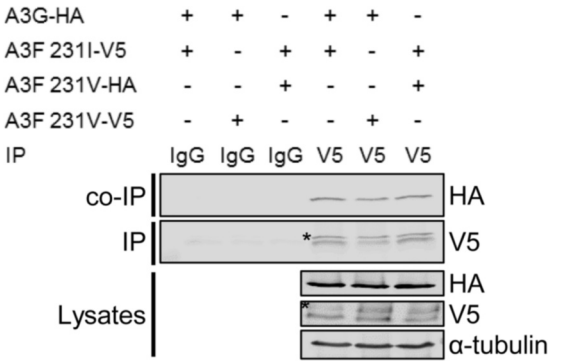

Fig. 3. A3F 231V and A3F 231I can interact in cells. The immunoprecipitation from cell lysates used either anti-V5 antibody or rabbit IgG (mock). Co-immunoprecipitation of A3F 231V-HA with A3F 231I-V5 or A3G-HA with A3F 231V-V5 and A3F 231I-V5 was detected through the HA tag. The presence of the V5-tagged protein in the co-immunoprecipitation samples is also shown. The experimental and mock samples were from the same lysate. The lysate blot demonstrates the cellular expression of α-tubulin, HA, and V5. A nonspecific band in the V5 blot is marked with an asterisk.

combination with A3G (Fig. 4A). These data extend previous data that demonstrated enhanced restriction of HIV-1 when A3G and A3F are coexpressed (Ara et al., 2017; Desimmie et al., 2016; Liddament et al., 2004). Notably, the V5-tagged versions of A3F 231I and A3F 231 V were able to decrease HIV-1 infectivity more than the untagged proteins (Figs. 1A and 4A), but the difference in restriction between the two A3F variants was the same (Fig. 1A, 50 ng, 1.6-fold, $p \leq 0.01$; Fig. 4A, 50 ng, 1.5-fold, $p \leq 0.001$). We also coexpressed A3F 231I-V5 and A3F 231V-HA (A3F 231I/A3F 231 V) and found that the decrease in HIV-1 infectivity was 2-fold ($p \leq 0.05$) and 1.5-fold ($p \leq 0.001$) more than each A3F alone, respectively. These data suggest that the weaker restriction activity of A3F 231I does not negatively affect the stronger restriction activity of A3F 231 V. In addition, in the presence of Vif, coexpressed A3F 231 V/A3F 231I was able to partially restrict HIV-1 (Fig. 4A, $p \leq 0.01$).

Immunoblotting of cell and virion lysates from the infectivity experiments demonstrated that the A3F 231 V resulted in increased steady state levels and encapsidation of coexpressed proteins, A3F 231I or A3G. Since each coexpression condition had an HA- and V5- tagged A3, samples from the same cell lysate had to be detected on separate V5 (Fig. 4B) or HA (Fig. 4C) blots. In both the presence and absence of Vif, increased HIV-1 restriction correlated with increased steady state expression of A3F 231I-V5 when coexpressed with A3F 231V-HA (Fig. 4B). In the absence of Vif and the presence of A3F 231V-HA, the A3F 231I-V5 expression increased 8.4-fold (Fig. 4B). In the presence of Vif and A3F 231V-HA, the A3F 231I-V5 expression increased 2-fold (Fig. 4B). A3G-HA expression levels in cells were increased in the presence of A3F 231V-V5 by 1.5-fold in the absence of Vif and 5-fold in the presence of Vif (Fig. 4C). Effects on encapsidation were also observed in the presence of A3F 231 V. Consistent with the partial restriction ability of A3F 231 V/A3F 231I in the presence of Vif (Fig. 4A, 66% infectivity), there was encapsidation of coexpressed A3F 231I-V5 (Fig. 4B, detectable encapsidation) and A3F 231V-HA (Fig. 4C, 5-fold more) even in the presence of Vif. Although A3G-HA encapsidation in the presence (3-fold) and absence (5-fold) of Vif was increased when coexpressed with A3F 231V-V5, the HIV-1 infectivity in the presence of Vif was not decreased more than A3G-HA alone (Fig. 4A and C), consistent with previous results that Vif inhibits encapsidated A3G activity (Britan-Rosich et al., 2011; Feng et al., 2013). Altogether, the data indicate that when A3F 231 V is expressed, it can increase steady state levels and encapsidation of A3F 231I and A3G (Fig. 4B-C). Although there was no enhancement of A3G-HA encapsidation levels in the presence of A3F 231I-V5 (Fig. 4C), A3G-HA was able to enhance A3F 231I-V5 cellular expression 10-fold in the absence of Vif and 8-fold in

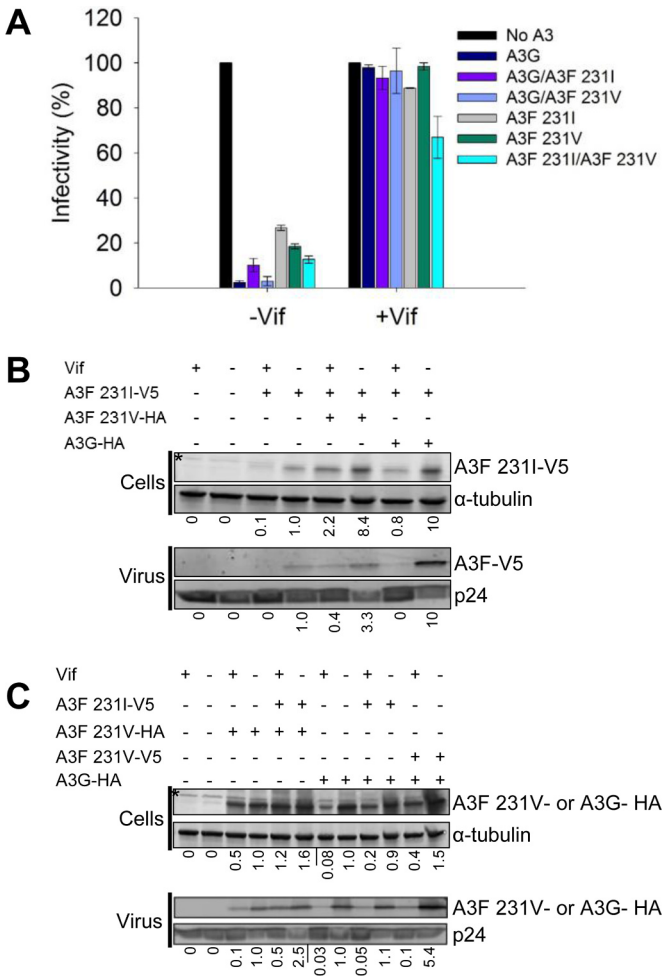

Fig. 4. Co-expression of A3F 231V and A3F 231I results in enhanced HIV-1 restriction ability. (A) HIV-1 infectivity was measured by β-galactosidase activity in reporter cells infected with ΔVif HIV-1 (-Vif) or HIV-1 (+Vif) that was produced in the absence or presence of A3G-HA, A3F 231V-V5, A3F 231V-HA, or A3F 231I-V5 in the combinations shown in the graph legend. There was always one V5- and one HA- tagged protein for each co-expression condition (see Materials and Methods). Error bars represent the standard deviations of the mean calculated from three independent experiments. (B) Immunoblotting with V5 antibody was used to detect cellular expression and virus encapsidation of A3F 231I-V5 in the presence of A3F 231V-HA or A3G-HA. (C) Immunoblotting with HA antibody was used to detect cellular expression and virus encapsidation of A3F 231V-HA or A3G-HA in the presence of A3F 231I-V5 or A3F 231V-V5. (B-C) Samples in these panels are from the same cell lysates. One representative blot from three independent experiments is shown. The A3 expression levels shown below blots were calculated by setting a –Vif condition for A3F 231I, A3F 231 V, or A3G to 1.0 and determining the relative values of other lanes. A nonspecific band in the V5 and HA blots was observed and is marked with an asterisk.

the presence of Vif (Fig. 4B). The presence of A3G-HA resulted in higher A3F 231I-V5 virion encapsidation levels in the absence of Vif (10-fold), but no change in the presence of Vif (Fig. 4B, A3F 231I-V5 not detectable). Altogether, these data demonstrate that different A3s can influence steady state cellular levels and virion encapsidation, with A3F 231 V having the highest effects.

2.6. In the presence and absence of Vif, coexpressed A3F 231V and A3F 231I induce more mutations in HIV-1 proviral DNA

To determine if the increased encapsidation of A3 enzymes resulted in increases in A3-induced mutations, we PCR amplified and sequenced

Table 3
Analysis of combined A3 expression on the induced mutagenesis in HIV-1 proviral DNA.

Virus Condition	A3 enzyme	Base pairs sequenced	G→A mutations (total)	GG→AG mutations (total)	GA→AA mutations (total)	G→A mutations (per kb)	GG→AG mutations (per kb)	GA→AA mutations (per kb)
-Vif	No A3	10881	0	0	0	0	0	0
	A3F 231V-V5	10530	27	1	26	2.56	0.09	2.47
	A3F 231I-V5	8073	15	1	14	1.86	0.12	1.73
	A3F 231V-HA/A3F 231I-V5	12285	45	1	44	3.66	0.08	3.58
	A3G-HA	6669	121	109	11	18.1	16.3	1.64
	A3G-HA/A3F 231V-V5	10530	172	102	70	16.3	9.69	6.64
	A3G-HA/ A3F 231I-V5	12987	134	95	39	10.3	7.32	3.00
+ Vif	No A3	11934	0	0	0	0	0	0
	A3F 231V-V5	10530	6	1	5	0.57	0.09	0.47
	A3F 231I-V5	10881	1	0	1	0.09	0	0.09
	A3F 231V-HA/A3F 231I-V5	11232	11	0	11	0.98	0	0.98

A 351 bp region of HIV-1 *protease* was PCR amplified from the three independent single-cycle replication assays shown in Fig. 4. Clones were sequenced, aligned with Clustal Omega (Sievers et al., 2011), and analyzed using Hypermut (Rose and Korber, 2000).

a 351 bp portion of HIV-1 *protease*. The data demonstrated that the tagged versions of A3F 231V-V5, A3F 231I-V5, and A3G-HA induced similar numbers of mutations to their untagged versions (+Vif and –Vif, Tables 1, 3). When the tagged A3F 231V-HA and A3F 231I-V5 were coexpressed and encapsidated into ΔVif HIV-1 virions, there was a 2-fold increase in mutations from A3F 231I-V5 alone and a 1.4-fold increase in mutations for A3F 231V-V5 alone (Table 3). The conditions where A3G-HA was coexpressed with an A3F-V5, in HIV-1 ΔVif producer cells, did not have significant increases in the numbers of mutations above A3G-HA alone, but when we examined the ratio of A3G-HA induced mutations to A3F-V5 induced mutations based on the mutational footprint, we observed a 2.7-fold (A3F 231 V) and 1.7-fold (A3F 231I) increase in A3F-induced mutations in the presence of A3G (Table 3). Of more significance was that in the presence of Vif, there was a 2-fold increase in mutations from the A3F 231 V alone condition (Table 3). Since A3F 231 V and A3F 231I have the same deamination motif, we could not discern which variant is more active. Based on analysis of encapsidation, since both had higher levels in virions (Fig. 4B and C), the deaminations could be due to both A3F variants.

3. Discussion

In HIV-1 genomes isolated from HIV-1 + individuals, there are mutational footprints in the (+) DNA at both 5′GG→5′AG and 5′GA→5′AA motifs (Bruner et al., 2016; de Lima-Stein et al., 2014; Eyzaguirre et al., 2013; Janini et al., 2001; Kieffer et al., 2005; Land et al., 2008; Ooms et al., 2013; Pace et al., 2006; Pathak and Temin, 1990; Piantadosi et al., 2009; Vartanian et al., 2002, 1991, 1994). The 5′GG→5′AG are clearly attributable to A3G (Yu et al., 2004). The origins of the 5′GA→5′AA mutations have been attributed to stable A3H haplotype (II, V, VII) induced mutations, due to an inability of some HIV-1 Vif variants to efficiently induce degradation of A3H (Ooms et al., 2013; Refsland et al., 2014). The role of A3D in inducing these mutations is known to be minor, but still significant (Chaipan et al., 2013; Dang et al., 2011; Duggal et al., 2011; Hultquist et al., 2011; Refsland et al., 2012). However, the role of A3F has been significant in some reports, but not others (Ara et al., 2014; Chaipan et al., 2013; Hultquist et al., 2011; Liddament et al., 2004; Miyagi et al., 2010; Mulder et al., 2010; Zennou and Bieniasz, 2006). In individual experiments with A3F, the mutational load is lower than A3G and A3H and this seemed incongruent with data demonstrating that A3F exerts a direct selective force on HIV-1 Vif and provides a protective effect in pretreatment HIV-1 cohorts (Adolph et al., 2018; Albin et al., 2010a; An et al., 2016; Ara et al., 2014; Feng et al., 2015; Zennou and Bieniasz, 2006). Here we provide a possible explanation for these data demonstrating that the A3F 231 V in comparison to the A3F 231I is more stable in cells, is partially protected from Vif-mediated degradation, is more highly encapsidated into virions, induces more mutations, and can increase encapsidation of coexpressed A3F 231I and A3G. These data suggest that the A3F 231 V through its own action and hetero-oligomerization with A3F 231I or A3G is a contributor to G→A mutations in HIV-1 + individuals.

A protective effect of A3F 231 V was demonstrated through genetic association analysis of pretreatment cohorts (An et al., 2016). Through this analysis it was shown that even when data were adjusted for known genetic factors (*HLA* allele and CCR5) the presence of even one A3F 231 V allele could significantly delay progression to clinical AIDS and lower viral load (An et al., 2016). The authors suggested that this was due to partial resistance of A3F 231 V to Vif, which had also been reported previously (An et al., 2016; Liddament et al., 2004). Here we show that the A3F 231 V is protected from Vif mediated degradation in cells more than A3F 231I and this results in more A3F 231 V encapsidation (Fig. 1). However, the A3F 231 V was not “resistant” to Vif mediated degradation, consistent with the 231 amino acid not being within the Vif binding interface (Albin et al., 2010b; Nakashima et al., 2016; Richards et al., 2015; Smith and Pathak, 2010). The protection

from Vif appears to be due to the higher steady state levels of A3F 231 V in cells due to enhanced stability (Figs. 1 and 2). Due to the high frequency of heterozygosity of the A3F 231 V and A3F 231I and the lack of sensitive native A3F antibodies, we were unable to demonstrate the higher expression of A3F 231 V in primary cells (Table 2 and data not shown). However, when equal amounts of A3F 231 V and A3F 231I were expressed in cells, the capacity of Vif to induce degradation of both enzymes was similar (Fig. 2B-C). Thus, the data suggest that the higher steady state levels of A3F in cells exceeds the degradation capacity of Vif. Despite the protective effect of A3F 231 V in HIV-1 + individuals (An et al., 2016), the partial protection of A3F 231 V from Vif mediated degradation resulted in at most a 20% decrease in infectivity in a Vif + HIV-1 single-cycle replication experiment (Fig. 1B). More consistent with the An *et al.* study was 4-fold more G→A mutations induced by A3F 231 V than A3F 231I in the presence of Vif (Table 1) (An et al., 2016). These small effects in our cell-based studies are similar to data available for the A3G H186R polymorphism. The A3G H186R polymorphism results in only a 2-fold decrease in A3G processivity and mutations induced in an in vitro assay (Feng and Chelico, 2011), but is nonetheless linked with faster progression to AIDS in HIV-1 + individuals (An et al., 2004; Reddy et al., 2016). Altogether, the data suggest that these small differences identified in cell culture can have an effect in HIV-1 + individuals. A possible explanation for this is that the small effects observed in cell-based studies become cumulative in multiple HIV-1 replication cycles. In addition or alternatively, the coexpression and hetero-oligomerization of A3 enzymes may amplify this effect. The coexpression of A3F 231 V and A3F 231I increased the encapsidation of both A3F variants in the presence of Vif and resulted in a corresponding 2-fold increase in A3F 231 V mutations and infectivity of 66% (Fig. 4B, C, and Table 3). Our data and previous analysis demonstrate that there are synergies between A3 enzymes that can enhance anti-HIV-1 activity, either directly due to changes in the biochemical characteristics of the enzymes or due to enhanced encapsidation in the presence of Vif (Fig. 4) (Ara et al., 2017). Despite observations that A3F 231 V on its own is partially protected from Vif-mediated degradation and our observation that A3F 231 V appears to protect A3G from Vif-mediated degradation, the mechanism is not known (An et al., 2016; Liddament et al., 2004).

Further, the reason for the stability differences between A3F 231 V and A3F 231I remain to be elucidated. Consistent with our observations, a nucleotide variant prediction model suggested that the A3F linked SNPs can have an effect on stability (Figs. 1 and 2) (An et al., 2016). The amino acid 108 is on predicted helix 3 in the noncatalytic N-terminal domain (NTD) and the amino acid 231 is on β-strand 2 in the catalytic C-terminal domain (Bohn et al., 2013; Feng et al., 2014; Nakashima et al., 2016; Siu et al., 2013). Neither of these structures are near the catalytic center, predicted nucleic acid binding motifs, or the Vif interface (Bohn et al., 2013; Feng et al., 2014; Nakashima et al., 2016; Richards et al., 2015; Siu et al., 2013). Although V231I is a conservative amino acid change, a Val to Ile amino acid change in other proteins, e.g., transthyretin, has been found to destabilize equilibrium kinetics of oligomerization and result in physiological dysfunction (Jiang et al., 2001). The A108S is a nonpolar to polar amino acid change and the Ser can form hydrogen bonds, unlike Ala, which may alter protein stability (Nelson et al., 2008).

4. Conclusions

Our data demonstrate that the A3F 231 V has higher steady state expression levels in cells and virion encapsidation than A3F 231I, in the presence and absence of Vif. This results in larger decreases in HIV-1 infectivity and higher mutation rates. The disruption of Vif-mediated degradation through hetero-oligomerization of A3s may be an example of increasing host restriction factor diversity to combat virus evolution (Compton et al., 2013; Meyerson and Sawyer, 2011). Altogether, this supports a model in which not only the genetic diversity of the host for each A3, but the ability of these A3s to functionally interact can contribute to a diverse and multifaceted protective response during HIV-1 infection.

5. Materials and methods

5.1. Plasmids and transfection conditions

To express two A3 enzymes on a single-cell level, the pVIVO2 plasmid (Invivogen) that contains two transcriptional units was used. For comparison to double expression experiments, pVIVO2 was also used to express tagged single A3 enzymes. The cloning of A3G-HA, A3F 108 S/231I-V5, and A3G-HA/A3F 108 S/231I-V5 into pVIVO2 was previously described (Ara et al., 2017). The pcDNA A3F 108 A/231 V was kindly provided by Reuben Harris (University of Minnesota) and subcloned into pVIVO2 using the same cloning strategy as previously reported to create A3F 108 A/231V-V5, A3F 108 A/231V-HA, A3G-HA/A3F 108 A/231V-V5, and A3F 108 A/231V-HA/A3F 108 S/231I-V5 (Ara et al., 2017). Primer sequences are available upon request. Untagged constructs of A3G, A3F 108 S/231I, and A3F 108 A/231 V were expressed from pcDNA and were previously reported (Ara et al., 2014; Liddament et al., 2004). Since the A3F polymorphisms at 108 and 231 are in strong linkage disequilibrium, for brevity we referred to the A3F forms as either 231I or 231 V (An et al., 2016; Duggal et al., 2013; Mulder et al., 2010; Zerbino et al., 2018).

5.2. Single-cycle replication assays

VSV-G pseudotyped HIV-1 LAI ΔVif ΔEnv were produced by transfecting 1×10^5 293 T cells per well of a 12-well plate. The 293 T cells were maintained in DMEM with 10% FBS. GeneJuice (Novagen) transfection reagent was used as per manufacturer's protocol. Cells were transfected with 500 ng of pHIV-1 LAI ΔVif ΔEnv, 180 ng of pMDG, which expresses VSV-G (Langlois et al., 2005; Naldini et al., 1996), and 25, 50, or 100 ng of A3 expression plasmid. The following pVIVO2 constructs were transfected for expression of tagged A3s: A3G-HA, A3F 231V-V5, A3F 231I-V5, A3G-HA/A3F 231I-V5, A3G-HA/A3F 231V-V5, and A3F 231V-HA/A3F 231I-V5. The following pcDNA3 constructs were transfected for expression of untagged A3s: A3G, A3F 231 V, and A3F 231I. To equalize the amount of plasmid DNA transfected, empty pVIVO2 or pcDNA3 vectors were used. After 24 h the media was changed and virus containing supernatants were harvested 24 h after the media change. Supernatants were filtered through a 0.45 μm polyvinylidene difluoride (PVDF) syringe filter.

For infection of a reporter cell line to determine infectivity 1×10^4 cells per well of a 96-well plate containing either HeLa CD4 + HIV-1 LTR-β-gal (MAGI) or TZM-Bl cells were infected with a serial dilution of virus normalized by p24 levels (QuickTiter Lentivirus Titer Kit, Cell Biolabs Inc.) in the presence of 8 μg/mL polybrene. Forty-eight hours after infection the cells were washed with PBS and infectivity was measured through colorimetric detection using a β-galactosidase assay reagent (Pierce) and spectrophotometer. Infectivity of each virus was compared by using the infectivity of the No A3 condition as 100%. Statistical significance of results was determined using a one-way random ANOVA.

5.3. Quantitative immunoblotting

293 T cells expressing No A3, A3G-HA, A3F 231V-V5, A3F 231I-V5, A3F-231V-HA, A3G-HA/A3F 231I-V5, A3G-HA/A3F 231V-V5, and A3F 231V-HA/A3F 231I-V5 from the single-cycle infectivity assays were detected using rabbit anti-HA (1:1000, Sigma) or rabbit anti-V5 (1:500, Sigma). 293 T cells expressing No A3 or untagged A3G, A3F 231 V, or A3F 231I were detected with ApoC17 rabbit antiserum (1:1000; Cat# 10082, NIH AIDS Reagent Program) for A3G or rabbit anti-APOBEC3F antibody, C-term (1:500; Cat# GTX47211, Genetex) for A3F (Holmes

et al., 2007; Kao et al., 2004). A3s were detected in cell lysates and virions. Cells were lysed using 2x Laemmli Buffer and 40 μg total protein was used. Virus was concentrated using Retro-X (Clontech) following the manufacturer's protocol and 20 μL of concentrated virus was used. Loading controls for cell lysates (α-tubulin, Sigma) and virus (p24, Cat #3537, NIH AIDS Reagent Program) were detected with mouse monoclonal antibodies. Secondary detection was performed using Licor IRDye antibodies produced in goat (IRDye 680-labeled anti-rabbit and IRDye 800-labeled anti mouse).

To detect Vif-mediated degradation of A3s, 1×10^5 293 T cells per well of a 24-well plate were transfected with 50 ng of A3F 231I-V5, 10 ng A3F 231V-V5, or empty pVIVO2 (No A3) and a titration of Vif_{LAI} expression plasmid (0,10, 25, 50, 100, and 200 ng). A 5-fold greater amount of A3F 231I was required to equalize the expression of both A3Fs. GeneJuice (Novagen) transfection reagent was used as described by the manufacturer. The media (DMEM and 10% FBS) was changed 24 h after the transfection. The cells were harvested 24 h after the media change with 2x Laemmli buffer and 40 μg total protein was used. Vif was detected with HIV-1 Vif monoclonal antibody (1:1000; Cat# 6459, NIH AIDS Reagent Program), followed by incubation with secondary goat anti-mouse IRDye 680-labeled. The V5-tagged A3F and α-tubulin was detected as described above.

Immunoblots were quantitatively analyzed where indicated in figures. Quantitation of band intensities was performed using Odyssey Software with normalization of each experimental lane to its respective α-tubulin or p24, which was detected in parallel on the same blot. Relative expression levels were then determined by comparison to a control sample set at 1.

5.4. Cycloheximide treatment

To determine protein stability in 293 T cells, 1×10^5 cells per mL were plated in each well of a 12-well plate. The cells were maintained in DMEM with 10% FBS. After 16 h the cells were transfected with A3F 231V-V5, A3F 231I-V5, or pVIVO2 empty vector expression plasmid. GeneJuice (Novagen) transfection reagent was used as per manufacturer's protocol. Twenty-four hours after the transfection, the media was changed. Thirty-six hours post transfection the media was replaced with cycloheximide containing media (100 μg/mL, Sigma). Cells were harvested and lysed in 2x Laemmli buffer at the following time points post cycloheximide addition: 0, 1, 2, 4, 6, 8, and 10 h. Protein stability was detected by quantitative immunoblotting as described above.

5.5. Co-immunoprecipitation assay

The co-immunoprecipitation method was previously described (Ara et al., 2017; Baig et al., 2014). In brief, 2.5×10^6 293 T cells per 75 cm^2 flask were transfected with 1 μg total DNA using GeneJuice (Novagen) as per manufacturer instructions. The plasmids transfected expressed A3G-HA/A3F 231I-V5, A3G-HA/A3F 231V-V5 or A3F 231V-HA/A3F-231I-V5. Each cell lysate was split into two fractions that were either used in a co-immunoprecipitation with nonspecific mouse IgG (mock) or the mouse anti-V5 (experiment). The co-immunoprecipitations were conducted in the presence of RNase A (Ara et al., 2017). A mouse anti-V5 (1:1000, Sigma) was used for immunoprecipitations and proteins were detected on the membrane using the same V5 antibody, mouse anti-HA (1:1000, Sigma), and polyclonal rabbit anti-α-tubulin (1:1000; Sigma). Secondary antibodies used were Licor IRDye antibodies 800-labeled goat anti-mouse and 680-labeled goat anti-rabbit secondary antibody.

5.6. Sequencing of integrated proviral DNA

For proviral sequencing, 1 $x10^5$ 293 T cells per well of a 24-well plate were infected with supernatant containing virus in the presence of 8 μg/mL polybrene. The plates were spinoculated at 800 x*g* for 1 h. Cells were harvested after 48 h by removing the media, washing with PBS, and lysing the cells and extracting DNA with DNAzol (Invitrogen). The PCR amplification of the *protease* region of HIV-1 (351 bp) and treatment of DNA with *Dpn*I was carried out as previously described (Ara et al., 2014). Sequences were analyzed with Clustal Omega (Sievers et al., 2011) and Hypermut (Rose and Korber, 2000).

Acknowledgements

This research was supported by a Canadian Institutes for Health Research Grant MOP-137090. The authors thank Ayan Moallin and Stephen Patrick for technical assistance. The following reagents were obtained through the NIH AIDS Reagent Program, Division of AIDS, NIAID, NIH: anti-ApoC17 from Dr. Klaus Strebel (Cat# 10082), Vif monoclonal antibody (Cat# 6459) from Dr. Michael H. Malim, and Anti-HIV-1 p24 Monoclonal (183-H12-5C) (Cat# 3537) from Dr. Bruce Chesebro and Kathy Wehrly.

References

Adolph, M.B., Ara, A., Feng, Y., Wittkopp, C.J., Emerman, M., Fraser, J.S., Chelico, L., 2017. Cytidine deaminase efficiency of the lentiviral viral restriction factor APOBEC3C correlates with dimerization. Nucleic Acids Res. 45, 3378–3394.

Adolph, M.B., Love, R.P., Chelico, L., 2018. Biochemical basis of APOBEC3 deoxycytidine deaminase activity on diverse DNA substrates. ACS Infect. Dis. 4, 224–238.

Albin, J.S., Hache, G., Hultquist, J.F., Brown, W.L., Harris, R.S., 2010a. Long-term restriction by APOBEC3F selects human immunodeficiency virus type 1 variants with restored Vif function. J. Virol. 84, 10209–10219.

Albin, J.S., LaRue, R.S., Weaver, J.A., Brown, W.L., Shindo, K., Harjes, E., Matsuo, H., Harris, R.S., 2010b. A single amino acid in human APOBEC3F alters susceptibility to HIV-1 Vif. J. Biol. Chem. 285, 40785–40792.

Alteri, C., Surdo, M., Bellocchi, M.C., Saccomandi, P., Continenza, F., Armenia, D., Parrotta, L., Carioti, L., Costa, G., Fourati, S., Di Santo, F., Scutari, R., Barbaliscia, S., Fedele, V., Carta, S., Balestra, E., Alcaro, S., Marcelin, A.G., Calvez, V., Ceccherini-Silberstein, F., Artese, A., Perno, C.F., Svicher, V., 2015. Incomplete APOBEC3G/F neutralization by HIV-1 vif mutants facilitates the genetic evolution from CCR5 to CXCR4 usage. Antimicrob. Agents Chemother. 59, 4870–4881.

An, P., Bleiber, G., Duggal, P., Nelson, G., May, M., Mangeat, B., Alobwede, I., Trono, D., Vlahov, D., Donfield, S., Goedert, J.J., Phair, J., Buchbinder, S., O'Brien, S.J., Telenti, A., Winkler, C.A., 2004. APOBEC3G genetic variants and their influence on the progression to AIDS. J. Virol. 78, 11070–11076.

An, P., Penugonda, S., Thorball, C.W., Bartha, I., Goedert, J.J., Donfield, S., Buchbinder, S., Binns-Roemer, E., Kirk, G.D., Zhang, W., Fellay, J., Yu, X.F., Winkler, C.A., 2016. Role of APOBEC3F gene variation in HIV-1 disease progression and pneumocystis pneumonia. PLoS Genet. 12, e1005921.

Apolonia, L., Schulz, R., Curk, T., Rocha, P., Swanson, C.M., Schaller, T., Ule, J., Malim, M.H., 2015. Promiscuous RNA binding ensures effective encapsidation of APOBEC3 proteins by HIV-1. PLoS Pathog. 11, e1004609.

Ara, A., Love, R.P., Chelico, L., 2014. Different mutagenic potential of HIV-1 restriction factors APOBEC3G and APOBEC3F is determined by distinct single-stranded DNA scanning mechanisms. PLoS Pathog. 10, e1004024.

Ara, A., Love, R.P., Follack, T.B., Ahmed, K.A., Adolph, M.B., Chelico, L., 2017. Mechanism of enhanced HIV restriction by virion coencapsidated cytidine deaminases APOBEC3F and APOBEC3G. J. Virol. 91.

Baig, T.T., Feng, Y., Chelico, L., 2014. Determinants of efficient degradation of APOBEC3 restriction factors by HIV-1 vif. J. Virol. 88, 14380–14395.

Bohn, M.F., Shandilya, S.M., Albin, J.S., Kouno, T., Anderson, B.D., McDougle, R.M., Carpenter, M.A., Rathore, A., Evans, L., Davis, A.N., Zhang, J., Lu, Y., Somasundaran, M., Matsuo, H., Harris, R.S., Schiffer, C.A., 2013. Crystal structure of the DNA cytosine deaminase APOBEC3F: the catalytically active and HIV-1 vif-binding domain. Structure 21, 1042–1050 (1993).

Britan-Rosich, E., Nowarski, R., Kotler, M., 2011. Multifaceted counter-APOBEC3G mechanisms employed by HIV-1 vif. J. Mol. Biol. 410, 1065–1076.

Bruner, K.M., Murray, A.J., Pollack, R.A., Soliman, M.G., Laskey, S.B., Capoferri, A.A., Lai, J., Strain, M.C., Lada, S.M., Hoh, R., Ho, Y.C., Richman, D.D., Deeks, S.G., Siliciano, J.D., Siliciano, R.F., 2016. Defective proviruses rapidly accumulate during acute HIV-1 infection. Nat. Med. 22, 1043–1049.

Chaipan, C., Smith, J.L., Hu, W.S., Pathak, V.K., 2013. APOBEC3G restricts HIV-1 to a greater extent than APOBEC3F and APOBEC3DE in human primary CD4+ T cells and macrophages. J. Virol. 87, 444–453.

Compton, A.A., Malik, H.S., Emerman, M., 2013. Host gene evolution traces the evolutionary history of ancient primate lentiviruses. Philos. Trans. R. Soc. Lond. B Biol. Sci. 368, 20120496.

Conticello, S.G., Harris, R.S., Neuberger, M.S., 2003. The Vif protein of HIV triggers degradation of the human antiretroviral DNA deaminase APOBEC3G. Curr. Biol. 13, 2009–2013.

Dang, Y., Wang, X., Esselman, W.J., Zheng, Y.H., 2006. Identification of APOBEC3DE as another antiretroviral factor from the human APOBEC family. J. Virol. 80, 10522–10533.

Dang, Y., Abudu, A., Son, S., Harjes, E., Spearman, P., Matsuo, H., Zheng, Y.H., 2011.

Identification of a single amino acid required for APOBEC3 antiretroviral cytidine deaminase activity. J. Virol. 85, 5691–5695.
Delviks-Frankenberry, K.A., Nikolaitchik, O.A., Burdick, R.C., Gorelick, R.J., Keele, B.F., Hu, W.S., Pathak, V.K., 2016. Minimal contribution of APOBEC3-induced G-to-A hypermutation to HIV-1 recombination and enetic variation. PLoS Pathog. 12, e1005646.
Desimmie, B.A., Burdick, R.C., Izumi, T., Doi, H., Shao, W., Alvord, W.G., Sato, K., Koyanagi, Y., Jones, S., Wilson, E., Hill, S., Maldarelli, F., Hu, W.S., Pathak, V.K., 2016. APOBEC3 proteins can copackage and comutate HIV-1 genomes. Nucleic Acids Res. 44, 7848–7865.
Duggal, N.K., Malik, H.S., Emerman, M., 2011. The breadth of antiviral activity of Apobec3DE in chimpanzees has been driven by positive selection. J. Virol. 85, 11361–11371.
Duggal, N.K., Fu, W., Akey, J.M., Emerman, M., 2013. Identification and antiviral activity of common polymorphisms in the APOBEC3 locus in human populations. Virology 443, 329–337.
Eyzaguirre, L.M., Charurat, M., Redfield, R.R., Blattner, W.A., Carr, J.K., Sajadi, M.M., 2013. Elevated hypermutation levels in HIV-1 natural viral suppressors. Virology 443, 306–312.
Feng, Y., Chelico, L., 2011. Intensity of deoxycytidine deamination of HIV-1 proviral DNA by the retroviral restriction factor APOBEC3G is mediated by the noncatalytic domain. J. Biol. Chem. 286, 11415–11426.
Feng, Y., Love, R.P., Chelico, L., 2013. HIV-1 viral infectivity factor (Vif) alters processive single-stranded DNA scanning of the retroviral restriction factor APOBEC3G. J. Biol. Chem. 288, 6083–6094.
Feng, Y., Baig, T.T., Love, R.P., Chelico, L., 2014. Suppression of APOBEC3-mediated restriction of HIV-1 by Vif. Front. Microbiol. 5, 450.
Feng, Y., Love, R.P., Ara, A., Baig, T.T., Adolph, M.B., Chelico, L., 2015. Natural Polymorphisms and Oligomerization of Human APOBEC3H Contribute to Single-stranded DNA Scanning Ability. J. Biol. Chem. 290, 27188–27203.
Grant, M., Larijani, M., 2017. Evasion of adaptive immunity by HIV through the action of host APOBEC3G/F enzymes. AIDS Res. Ther. 14, 44.
Guo, Y., Dong, L., Qiu, X., Wang, Y., Zhang, B., Liu, H., Yu, Y., Zang, Y., Yang, M., Huang, Z., 2014. Structural basis for hijacking CBF-beta and CUL5 E3 ligase complex by HIV-1 Vif. Nature 505, 229–233.
Harris, R.S., Dudley, J.P., 2015. APOBECs and virus restriction. Virology 479–480, 131–145.
Harris, R.S., Petersen-Mahrt, S.K., Neuberger, M.S., 2002. RNA editing enzyme APOBEC1 and some of its homologs can act as DNA mutators. Mol. Cell 10, 1247–1253.
Harris, R.S., Bishop, K.N., Sheehy, A.M., Craig, H.M., Petersen-Mahrt, S.K., Watt, I.N., Neuberger, M.S., Malim, M.H., 2003. DNA deamination mediates innate immunity to retroviral infection. Cell 113, 803–809.
Harris, R.S., Hultquist, J.F., Evans, D.T., 2012. The restriction factors of human immunodeficiency virus. J. Biol. Chem. 287, 40875–40883.
Holmes, M., Zhang, F., Bieniasz, P.D., 2015. single-cell and single-cycle analysis of HIV-1 replication. PLoS Pathog. 11, e1004961.
Holmes, R.K., Koning, F.A., Bishop, K.N., Malim, M.H., 2007. APOBEC3F can inhibit the accumulation of HIV-1 reverse transcription products in the absence of hypermutation. Comparisons with APOBEC3G. J. Biol. Chem. 282, 2587–2595.
Hultquist, J.F., Lengyel, J.A., Refsland, E.W., LaRue, R.S., Lackey, L., Brown, W.L., Harris, R.S., 2011. Human and rhesus APOBEC3D, APOBEC3F, APOBEC3G, and APOBEC3H demonstrate a conserved capacity to restrict Vif-deficient HIV-1. J. Virol. 85, 11220–11234.
Jager, S., Kim, D.Y., Hultquist, J.F., Shindo, K., LaRue, R.S., Kwon, E., Li, M., Anderson, B.D., Yen, L., Stanley, D., Mahon, C., Kane, J., Franks-Skiba, K., Cimermancic, P., Burlingame, A., Sali, A., Craik, C.S., Harris, R.S., Gross, J.D., Krogan, N.J., 2012. Vif hijacks CBF-beta to degrade APOBEC3G and promote HIV-1 infection. Nature 481, 371–375.
Janini, M., Rogers, M., Birx, D.R., McCutchan, F.E., 2001. Human immunodeficiency virus type 1 DNA sequences genetically damaged by hypermutation are often abundant in patient peripheral blood mononuclear cells and may be generated during near-simultaneous infection and activation of CD4(+) T cells. J. Virol. 75, 7973–7986.
Jern, P., Russell, R.A., Pathak, V.K., Coffin, J.M., 2009. Likely role of APOBEC3G-mediated G-to-A mutations in HIV-1 evolution and drug resistance. PLoS Pathog. 5, e1000367.
Jiang, X., Buxbaum, J.N., Kelly, J.W., 2001. The V122I cardiomyopathy variant of transthyretin increases the velocity of rate-limiting tetramer dissociation, resulting in accelerated amyloidosis. Proc. Natl. Acad. Sci. USA 98, 14943–14948.
Kao, S., Khan, M.A., Miyagi, E., Plishka, R., Buckler-White, A., Strebel, K., 2003. The human immunodeficiency virus type 1 Vif protein reduces intracellular expression and inhibits packaging of APOBEC3G (CEM15), a cellular inhibitor of virus infectivity. J. Virol. 77, 11398–11407.
Kao, S., Miyagi, E., Khan, M.A., Takeuchi, H., Opi, S., Goila-Gaur, R., Strebel, K., 2004. Production of infectious human immunodeficiency virus type 1 does not require depletion of APOBEC3G from virus-producing cells. Retrovirology 1, 27.
Kieffer, T.L., Kwon, P., Nettles, R.E., Han, Y., Ray, S.C., Siliciano, R.F., 2005. G– > A hypermutation in protease and reverse transcriptase regions of human immunodeficiency virus type 1 residing in resting CD4+ T cells in vivo. J. Virol. 79, 1975–1980.
Kim, E.Y., Lorenzo-Redondo, R., Little, S.J., Chung, Y.S., Phalora, P.K., Maljkovic Berry, I., Archer, J., Penugonda, S., Fischer, W., Richman, D.D., Bhattacharya, T., Malim, M.H., Wolinsky, S.M., 2014. Human APOBEC3 induced mutation of human immunodeficiency virus type-1 contributes to adaptation and evolution in natural infection. PLoS Pathog. 10, e1004281.
Kitamura, S., Ode, H., Nakashima, M., Imahashi, M., Naganawa, Y., Kurosawa, T., Yokomaku, Y., Yamane, T., Watanabe, N., Suzuki, A., Sugiura, W., Iwatani, Y., 2012. The APOBEC3C crystal structure and the interface for HIV-1 Vif binding. Nat. Struct. Mol. Biol. 19, 1005–1010.
Land, A.M., Ball, T.B., Luo, M., Pilon, R., Sandstrom, P., Embree, J.E., Wachihi, C., Kimani, J., Plummer, F.A., 2008. Human immunodeficiency virus (HIV) type 1 proviral hypermutation correlates with CD4 count in HIV-infected women from Kenya. J. Virol. 82, 8172–8182.
Langlois, M.A., Beale, R.C., Conticello, S.G., Neuberger, M.S., 2005. Mutational comparison of the single-domained APOBEC3C and double-domained APOBEC3F/G antiretroviral cytidine deaminases provides insight into their DNA target site specificities. Nucleic Acids Res. 33, 1913–1923.
Liddament, M.T., Brown, W.L., Schumacher, A.J., Harris, R.S., 2004. APOBEC3F properties and hypermutation preferences indicate activity against HIV-1 in vivo. Curr. Biol. 14, 1385–1391.
de Lima-Stein, M.L., Alkmim, W.T., Bizinoto, M.C., Lopez, L.F., Burattini, M.N., Maricato, J.T., Giron, L., Sucupira, M.C., Diaz, R.S., Janini, L.M., 2014. In vivo HIV-1 hypermutation and viral loads among antiretroviral-naive Brazilian patients. AIDS Res. Hum. Retrovir. 30, 867–880.
Mangeat, B., Turelli, P., Caron, G., Friedli, M., Perrin, L., Trono, D., 2003. Broad antiretroviral defence by human APOBEC3G through lethal editing of nascent reverse transcripts. Nature 424, 99–103.
Mangeat, B., Turelli, P., Liao, S., Trono, D., 2004. A single amino acid determinant governs the species-specific sensitivity of APOBEC3G to Vif action. J. Biol. Chem. 279, 14481–14483.
Mariani, R., Chen, D., Schrofelbauer, B., Navarro, F., Konig, R., Bollman, B., Munk, C., Nymark-McMahon, H., Landau, N.R., 2003. Species-specific exclusion of APOBEC3G from HIV-1 virions by Vif. Cell 114, 21–31.
Marin, M., Rose, K.M., Kozak, S.L., Kabat, D., 2003. HIV-1 Vif protein binds the editing enzyme APOBEC3G and induces its degradation. Nat. Med. 9, 1398–1403.
Meyerson, N.R., Sawyer, S.L., 2011. Two-stepping through time: mammals and viruses. Trends Microbiol. 19, 286–294.
Miyagi, E., Brown, C.R., Opi, S., Khan, M., Goila-Gaur, R., Kao, S., Walker Jr., R.C., Hirsch, V., Strebel, K., 2010. Stably expressed APOBEC3F has negligible antiviral activity. J. Virol. 84, 11067–11075.
Monajemi, M., Woodworth, C.F., Zipperlen, K., Gallant, M., Grant, M.D., Larijani, M., 2014. Positioning of APOBEC3G/F mutational hotspots in the human immunodeficiency virus genome favors reduced recognition by CD8+ T cells. PLoS One 9, e93428.
Mulder, L.C., Harari, A., Simon, V., 2008. Cytidine deamination induced HIV-1 drug resistance. Proc. Natl. Acad. Sci. USA 105, 5501–5506.
Mulder, L.C., Ooms, M., Majdak, S., Smedresman, J., Linscheid, C., Harari, A., Kunz, A., Simon, V., 2010. Moderate influence of human APOBEC3F on HIV-1 replication in primary lymphocytes. J. Virol. 84, 9613–9617.
Nakashima, M., Ode, H., Kawamura, T., Kitamura, S., Naganawa, Y., Awazu, H., Tsuzuki, S., Matsuoka, K., Nemoto, M., Hachiya, A., Sugiura, W., Yokomaku, Y., Watanabe, N., Iwatani, Y., 2016. Structural Insights into HIV-1 Vif-APOBEC3F Interaction. J. Virol. 90, 1034–1047.
Naldini, L., Blomer, U., Gallay, P., Ory, D., Mulligan, R., Gage, F.H., Verma, I.M., Trono, D., 1996. In vivo gene delivery and stable transduction of nondividing cells by a lentiviral vector. Science 272, 263–267.
Nelson, D., Lehninger, Albert L., Cox, Michael M., 2008. Lehninger Principles of Biochemistry, 5th ed. W.H. Freeman, New York.
OhAinle, M., Kerns, J.A., Li, M.M., Malik, H.S., Emerman, M., 2008. Antiretroelement activity of APOBEC3H was lost twice in recent human evolution. Cell Host Microbe 4, 249–259.
Ooms, M., Majdak, S., Seibert, C.W., Harari, A., Simon, V., 2010. The localization of APOBEC3H variants in HIV-1 virions determines their antiviral activity. J. Virol. 84, 7961–7969.
Ooms, M., Brayton, B., Letko, M., Maio, S.M., Pilcher, C.D., Hecht, F.M., Barbour, J.D., Simon, V., 2013. HIV-1 vif adaptation to human APOBEC3H haplotypes. Cell Host Microbe 14, 411–421.
Pace, C., Keller, J., Nolan, D., James, I., Gaudieri, S., Moore, C., Mallal, S., 2006. Population level analysis of human immunodeficiency virus type 1 hypermutation and its relationship with APOBEC3G and vif genetic variation. J. Virol. 80, 9259–9269.
Pathak, V.K., Temin, H.M., 1990. Broad spectrum of in vivo forward mutations, hypermutations, and mutational hotspots in a retroviral shuttle vector after a single replication cycle: substitutions, frameshifts, and hypermutations. Proc. Natl. Acad. Sci. USA 87, 6019–6023.
Piantadosi, A., Humes, D., Chohan, B., McClelland, R.S., Overbaugh, J., 2009. Analysis of the percentage of human immunodeficiency virus type 1 sequences that are hypermutated and markers of disease progression in a longitudinal cohort, including one individual with a partially defective vif. J. Virol. 83, 7805–7814.
Pollack, R.A., Jones, R.B., Pertea, M., Bruner, K.M., Martin, A.R., Thomas, A.S., Capoferri, A.A., Beg, S.A., Huang, S.H., Karandish, S., Hao, H., Halper-Stromberg, E., Yong, P.C., Kovacs, C., Benko, E., Siliciano, R.F., Ho, Y.C., 2017. Defective HIV-1 proviruses are expressed and can be recognized by Cytotoxic T Lymphocytes, which shape the proviral landscape. Cell Host Microbe 21 (494–506), e494.
Reddy, K., Ooms, M., Letko, M., Garrett, N., Simon, V., Ndung'u, T., 2016. Functional characterization of Vif proteins from HIV-1 infected patients with different APOBEC3G haplotypes. AIDS 30, 1723–1729.
Refsland, E.W., Hultquist, J.F., Harris, R.S., 2012. Endogenous origins of HIV-1 G-to-A hypermutation and restriction in the nonpermissive T cell line CEM2n. PLoS Pathog. 8, e1002800.
Refsland, E.W., Hultquist, J.F., Luengas, E.M., Ikeda, T., Shaban, N.M., Law, E.K., Brown, W.L., Reilly, C., Emerman, M., Harris, R.S., 2014. Natural polymorphisms in human

APOBEC3H and HIV-1 vif combine in primary T lymphocytes to affect viral G-to-A mutation levels and infectivity. PLoS Genet. 10, e1004761.
Richards, C., Albin, J.S., Demir, O., Shaban, N.M., Luengas, E.M., Land, A.M., Anderson, B.D., Holten, J.R., Anderson, J.S., Harki, D.A., Amaro, R.E., Harris, R.S., 2015. The binding interface between human APOBEC3F and HIV-1 Vif elucidated by genetic and computational approaches. Cell Rep. 13, 1781–1788.
Rose, P.P., Korber, B.T., 2000. Detecting hypermutations in viral sequences with an emphasis on G – > A hypermutation. Bioinformatics 16, 400–401.
Sato, K., Takeuchi, J.S., Misawa, N., Izumi, T., Kobayashi, T., Kimura, Y., Iwami, S., Takaori-Kondo, A., Hu, W.S., Aihara, K., Ito, M., An, D.S., Pathak, V.K., Koyanagi, Y., 2014. APOBEC3D and APOBEC3F potently promote HIV-1 diversification and evolution in humanized mouse model. PLoS Pathog. 10, e1004453.
Schrofelbauer, B., Chen, D., Landau, N.R., 2004. A single amino acid of APOBEC3G controls its species-specific interaction with virion infectivity factor (Vif). Proc. Natl. Acad. Sci. USA 101, 3927–3932.
Sheehy, A.M., Gaddis, N.C., Choi, J.D., Malim, M.H., 2002. Isolation of a human gene that inhibits HIV-1 infection and is suppressed by the viral Vif protein. Nature 418, 646–650.
Sheehy, A.M., Gaddis, N.C., Malim, M.H., 2003. The antiretroviral enzyme APOBEC3G is degraded by the proteasome in response to HIV-1 Vif. Nat. Med. 9, 1404–1407.
Sievers, F., Wilm, A., Dineen, D., Gibson, T.J., Karplus, K., Li, W., Lopez, R., McWilliam, H., Remmert, M., Soding, J., Thompson, J.D., Higgins, D.G., 2011. Fast, scalable generation of high-quality protein multiple sequence alignments using clustal omega. Mol. Syst. Biol. 7, 539.
Simon, V., Zennou, V., Murray, D., Huang, Y., Ho, D.D., Bieniasz, P.D., 2005. Natural variation in Vif: differential impact on APOBEC3G/3F and a potential role in HIV-1 diversification. PLoS Pathog. 1, e6.
Siu, K.K., Sultana, A., Azimi, F.C., Lee, J.E., 2013. Structural determinants of HIV-1 Vif susceptibility and DNA binding in APOBEC3F. Nat. Commun. 4, 2593.
Smith, J.L., Pathak, V.K., 2010. Identification of specific determinants of human APOBEC3F, APOBEC3C, and APOBEC3DE and African green monkey APOBEC3F that interact with HIV-1 Vif. J. Virol. 84, 12599–12608.
Squires, K.D., Monajemi, M., Woodworth, C.F., Grant, M.D., Larijani, M., 2015. Impact of APOBEC mutations on CD8+ T cell recognition of HIV epitopes varies depending on the restricting HLA. J. Acquir. Immune Defic. Syndr. 70, 172–178.
Stopak, K., de Noronha, C., Yonemoto, W., Greene, W.C., 2003. HIV-1 Vif blocks the antiviral activity of APOBEC3G by impairing both its translation and intracellular stability. Mol. Cell 12, 591–601.
Vartanian, J.P., Meyerhans, A., Asjö, B., Wain-Hobson, S., 1991. Selection, recombination, and G——A hypermutation of human immunodeficiency virus type 1 genomes. J. Virol. 65, 1779–1788.
Vartanian, J.P., Meyerhans, A., Sala, M., Wain-Hobson, S., 1994. G– > A hypermutation of the human immunodeficiency virus type 1 genome: evidence for dCTP pool imbalance during reverse transcription. Proc. Natl. Acad. Sci. USA 91, 3092–3096.
Vartanian, J.P., Henry, M., Wain-Hobson, S., 2002. Sustained G– > A hypermutation during reverse transcription of an entire human immunodeficiency virus type 1 strain Vau group O genome. J. Gen. Virol. 83, 801–805.
Wang, X., Abudu, A., Son, S., Dang, Y., Venta, P.J., Zheng, Y.H., 2011. Analysis of human APOBEC3H haplotypes and anti-human immunodeficiency virus type 1 activity. J. Virol. 85, 3142–3152.
Wiegand, H.L., Doehle, B.P., Bogerd, H.P., Cullen, B.R., 2004. A second human antiretroviral factor, APOBEC3F, is suppressed by the HIV-1 and HIV-2 Vif proteins. EMBO J. 23, 2451–2458.
Wittkopp, C.J., Adolph, M.B., Wu, L.I., Chelico, L., Emerman, M., 2016. A single nucleotide polymorphism in human APOBEC3C enhances restriction of lentiviruses. PLoS Pathog. 12, e1005865.
Xu, H., Svarovskaia, E.S., Barr, R., Zhang, Y., Khan, M.A., Strebel, K., Pathak, V.K., 2004. A single amino acid substitution in human APOBEC3G antiretroviral enzyme confers resistance to HIV-1 virion infectivity factor-induced depletion. Proc. Natl. Acad. Sci. USA 101, 5652–5657.
York, A., Kutluay, S.B., Errando, M., Bieniasz, P.D., 2016. The RNA binding specificity of human APOBEC3 proteins resembles That of HIV-1 nucleocapsid. PLoS Pathog. 12, e1005833.
Yu, Q., Konig, R., Pillai, S., Chiles, K., Kearney, M., Palmer, S., Richman, D., Coffin, J.M., Landau, N.R., 2004. Single-strand specificity of APOBEC3G accounts for minus-strand deamination of the HIV genome. Nat. Struct. Mol. Biol. 11, 435–442.
Yu, X., Yu, Y., Liu, B., Luo, K., Kong, W., Mao, P., Yu, X.F., 2003. Induction of APOBEC3G ubiquitination and degradation by an HIV-1 Vif-Cul5-SCF complex. Science 302, 1056–1060.
Zennou, V., Bieniasz, P.D., 2006. Comparative analysis of the antiretroviral activity of APOBEC3G and APOBEC3F from primates. Virology 349, 31–40.
Zerbino, D.R., Achuthan, P., Akanni, W., Amode, M.R., Barrell, D., Bhai, J., Billis, K., Cummins, C., Gall, A., Giron, C.G., Gil, L., Gordon, L., Haggerty, L., Haskell, E., Haggerty, T., Izuogu, O.G., Janacek, S.H., Juettemann, T., To, J.K., Laird, M.R., Lavidas, I., Liu, Z., Loveland, J.E., Maurel, T., McLaren, W., Moore, B., Mudge, J., Murphy, D.N., Newman, V., Nuhn, M., Ogeh, D., Ong, C.K., Parker, A., Patricio, M., Riat, H.S., Schuilenburg, H., Sheppard, D., Sparrow, H., Taylor, K., Thormann, A., Vullo, A., Walts, B., Zadissa, A., Frankish, A., Hunt, S.E., Kostadima, M., Langridge, N., Martin, F.J., Muffato, M., Perry, E., Ruffier, M., Staines, D.M., Trevanion, S.J., Aken, B.L., Cunningham, F., Yates, A., Flicek, A., 2018. Ensembl 2018. Nucleic Acids Res. 46, D754–D761.
Zhang, H., Yang, B., Pomerantz, R.J., Zhang, C., Arunachalam, S.C., Gao, L., 2003. The cytidine deaminase CEM15 induces hypermutation in newly synthesized HIV-1 DNA. Nature 424, 94–98.
Zhang, W., Du, J., Evans, S.L., Yu, Y., Yu, X.F., 2011. T-cell differentiation factor CBF-beta regulates HIV-1 Vif-mediated evasion of host restriction. Nature 481, 376–379.
Zheng, Y.H., Irwin, D., Kurosu, T., Tokunaga, K., Sata, T., Peterlin, B.M., 2004. Human APOBEC3F is another host factor that blocks human immunodeficiency virus type 1 replication. J. Virol. 78, 6073–6076.